

Figure S1: γ KCs have strong lateral axo-axonal connections and express mAChR-B. Related to Figure 1.

A. Dendritic (left) and axonal (right) lateral KC-KC connections, note different scale. The number of synapses made between each KC to all other KCs, arranged by the three main subclasses of KCs, in the different regions of the MB (Calyx and Lobes) are shown. KCs show strong axonal connections to other cognate KCs. Blue ($\alpha'\beta'$), red ($\alpha\beta$) and yellow (γ), indicate the KC subtypes as designated.

B. The number of post-synaptic KCs each KC has according to the different types of KCs. Blue, red and yellow, indicate the KC subtypes as designated.

C. Mean number of post-synaptic KCs, obtained from the data presented in B. Blue, red and yellow, indicate the KC subtypes as designated. γ KCs have the highest number of post-synaptic KC partners (mean \pm SEM), n (left to right): 337, 889, 689; **** $p < 0.0001$; (Kruskal-Wallis Dunn's correction for multiple comparisons. For detailed statistical analysis see **Table S1**).

D. Data from Davie et al., 2018. 56,902 *Drosophila* brain cells arranged according to their single-cell transcriptome profiles, along the top 2 principal components using t-SNE. Red coloring indicates expression of mAChR-B. KC subtype clusters are labeled as identified in Davie et al., 2018.

E. As in A but with data from Croset et al., 2018 (10,286 *Drosophila* brain cells).

F. Data from Aso et al. 2019. (2500 γ and $\alpha\beta$ KCs, 1000 $\alpha'\beta'$ KCs). Blue ($\alpha'\beta'$), red ($\alpha\beta$) and yellow (γ), indicate the KC subtypes as designated.

For A, B, Images screenshotted from SCoPe (<http://scope.aertslab.org>) on 9 March 2022.

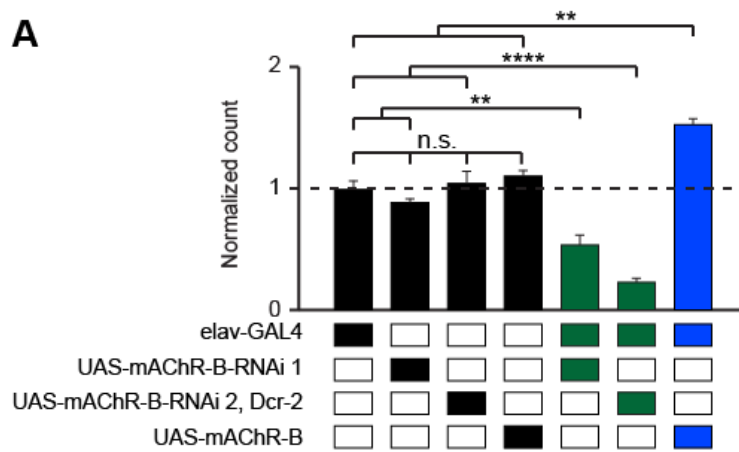
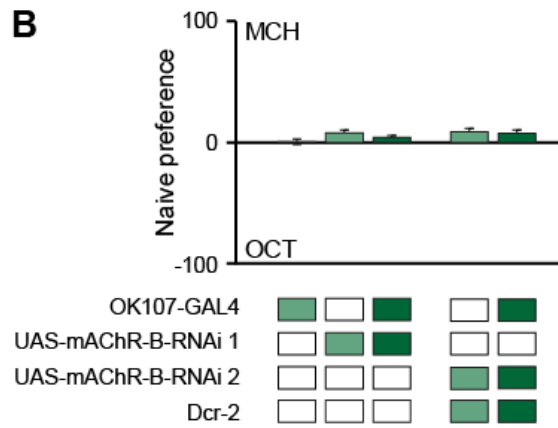
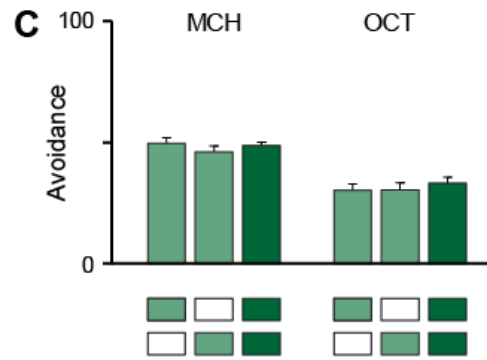
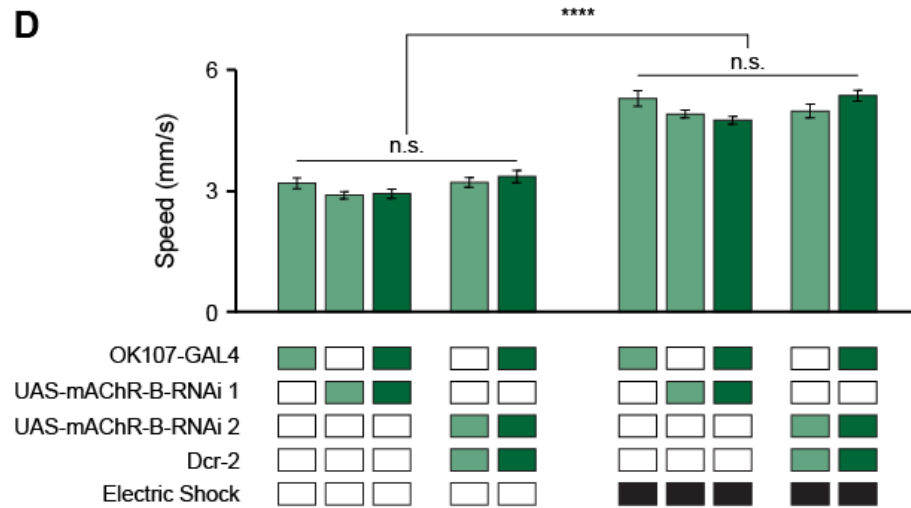
A**B****C****D**

Figure S2: Control Experiments for mAChR-B RNAi efficiency and behavior experiments. Related to Figure 2.

A. qRT-PCR of mAChR-B with both UAS-mAChR-B RNAi (RNAi 1 and 2) and with UAS-mAChR-B driven by elav-GAL4. The housekeeping gene β -Tubulin was used for normalization. All groups are normalized to elav-GAL4. Knockdown flies have ~55% and 25% for RNAi 1 and 2 respectively and overexpression of mAChR-B has ~155% of the control levels of mAChR-B mRNA (mean \pm SEM; 3 biological replicates each with 3 technical replicates; * $p < 0.05$; (one way ANOVA with Holm-Šidák correction for multiple comparisons). For detailed statistical analysis see **Table S1**.

B. mAChR-B KD flies show normal preference between OCT and MCH compared to their genotypic controls (mean \pm SEM), n (left to right): 56, 162, 77, 66, 61 (Welch and Brown-Forsythe tests- Dunnett's multiple comparisons test). For detailed statistical analysis see **Table S1**.

C. mAChR-B KD flies show normal olfactory avoidance of OCT and MCH compared to their genotypic controls (mean \pm SEM), n (left to right): MCH: 96, 96, 88; OCT: 108, 75, 95 (Kruskal-Wallis Dunn's correction for multiple comparisons). For detailed statistical analysis see **Table S1**.

D. Sensitivity to shock (extent to which flies walk faster while being shocked) is not affected by knocking down mAChR-B in KCs. Walking speed with (right) or without (left) an electric shock is presented. mAChR-B KD did not affect walking speed in either condition (mean \pm SEM, n (left to right): no shock: 49, 162, 77, 66, 61; with shock: 49, 162, 77, 66, 61 (Kruskal-Wallis Dunn's correction for multiple comparisons). For detailed statistical analysis see **Table S1**.

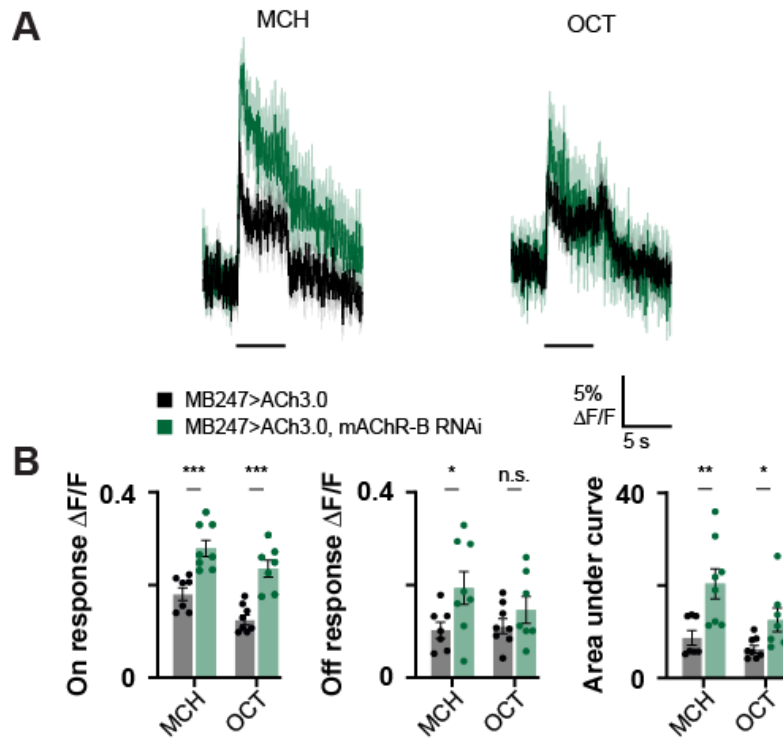


Figure S3: mAChR-B KD increase γ KC synaptic release. Related to Figure 3.

Synaptic release as indicated by ACh signal in KCs following MCH or OCT was measured in control flies (MB247-GAL4>UAS-GACh3.0) and KD flies (MB247-GAL4>UAS-GACh3.0, UAS-mAChR-B).

A. $\Delta F/F$ of GACh3.0 signal in the lobe of γ KCs for control (black) and KD (green) flies, during presentation of odor pulses (horizontal lines). Data are mean (solid line) \pm SEM (shaded area).

B. Peak “on” response (left), Peak “off” response (middle), and the integral of the odor response (right) of the traces presented in A (mean \pm SEM). n for control and KD flies, respectively: MCH, 7, 8; OCT, 8, 7. * $p < 0.05$, ** $p < 0.01$, (Mann-Whitney test with Holm Šidák correction for multiple comparisons). For detailed statistical analysis see **Table S1**.

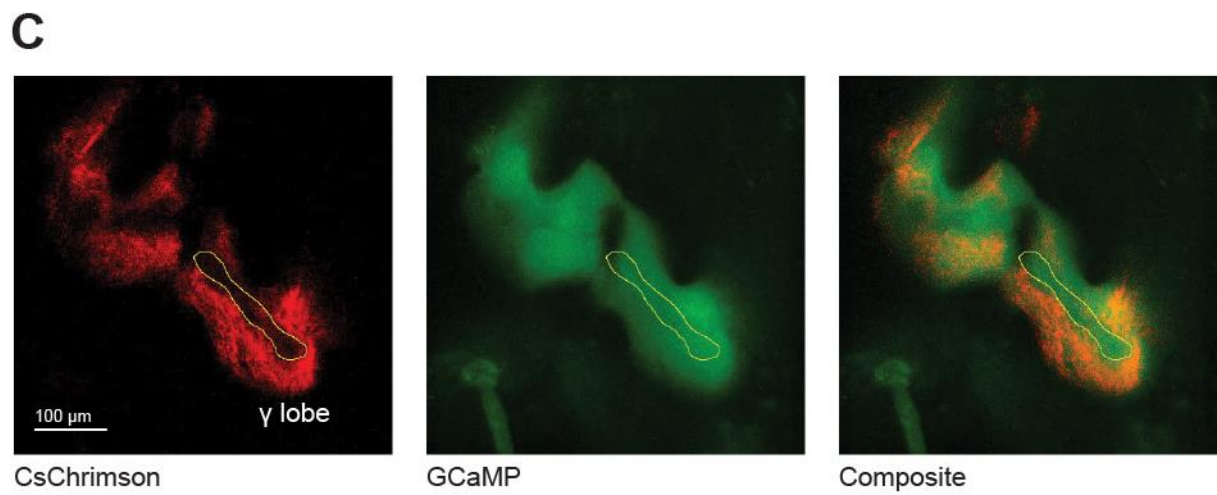
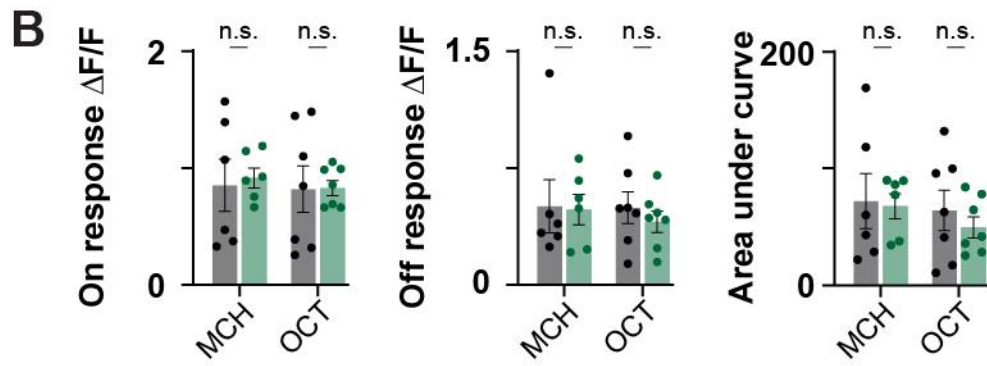
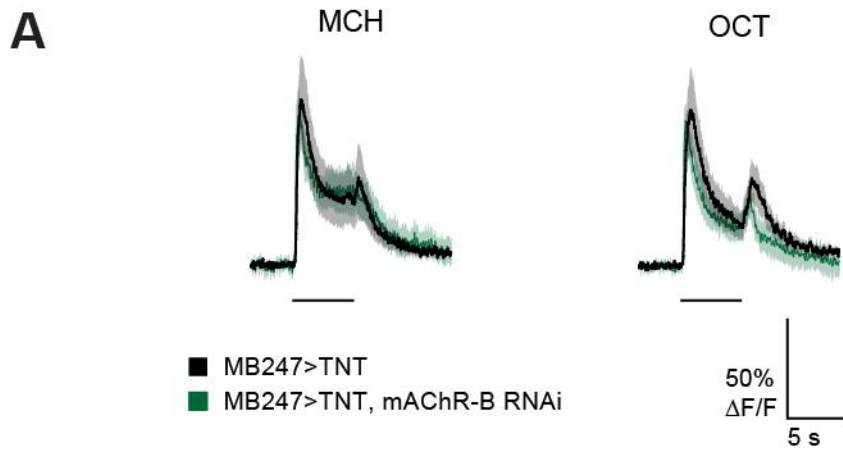


Figure S4: mAChR-B effect is post-synaptic to KC release. Related to Figure 6.

KC odor responses to MCH and OCT were measured in control flies (MB247-GAL4>UAS-GCaMP6f) and knockdown flies (MB247-GAL4>UAS-GCaMP6f, UAS-mAChR-B RNAi 1) when KC synaptic release was blocked using UAS-TNT.

A. $\Delta F/F$ of GCaMP6f signal in the lobe of γ KCs for control (black) and KD (green) flies, during presentation of odor pulses (horizontal lines). Data are mean (solid line) \pm SEM (shaded area).

B. Peak “on” response (left), Peak “off” response (middle), and the integral of the odor response (right) of the traces presented in A (mean \pm SEM). n for control and KD flies, respectively: MCH, 6, 6; OCT, 7, 7. No statistical difference is observed between control and mAChR-KD flies (Mann-Whitney test with Holm Šidák correction for multiple comparisons). For detailed statistical analysis see **Table S1**.

C. Example of region selection for the analysis presented in Figure 5. A single plane average intensity projection over time (500 frames) of a 2-photon image obtained from a fly carrying MB247-LexA-LexAop-GCaMP6f, and CsChrimson::tdTomato in stochastically distributed subsets of neurons using TI{20XUAS-SPARC2-I-Syn21-CsChrimson::tdTomato-3.1}CR-P40 within the MB247-GAL4 driver line transgenes. ROIs were selected manually in Fiji to include only GCaMP labeled areas and not tdTomato. *Left*, CsChrimson is only partially expressed in the γ lobe. *Middle*, GCaMP6f signal throughout the γ lobe. *Right*, a composite of the CsChrimson and GCaMP6f signals.

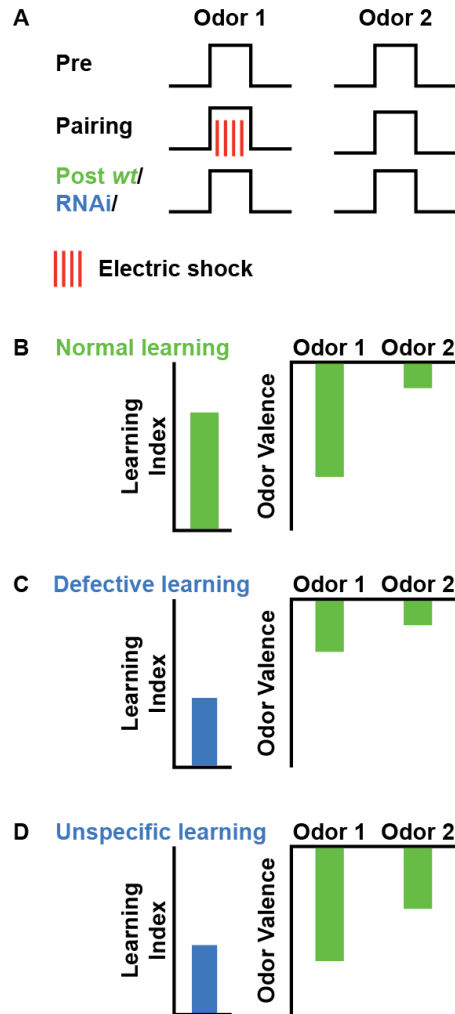


Figure S5: Comparison between defective and unspecific learning. Related to Figure 7.

A. Illustration of the classical conditioning protocol. The preference between odor 1 and odor 2 is evaluated prior to conditioning. Odors are then subjected to a conditioning protocol in which odor 1 (CS⁺) is associated with an electric shock. This is then followed by another examination of odor preference.

B. Under normal conditions following conditioning, the valence of odor 1 (CS⁺) becomes very negative whereas that of odor 2 (CS⁻) is not affected.

C. When defective conditioning occurs, for example in the case where the dopaminergic neurons are inactive or when the dopaminergic receptors on KCs are knocked down, odor 1 (CS⁺) valence is not as negative as under normal conditions. Thus, the difference between the valence of odor 1 and odor 2 becomes smaller, and the learning index is reduced.

D. When unspecific conditioning occurs, as suggested following mAChR-B KD, the valence of odor 1 (CS⁺) becomes very negative, as under normal conditions. However, the valence of odor 2 (CS⁻) is also affected even if to a lesser extent. Thus, the difference between the valence of odor 1 and odor 2 becomes smaller and the learning index is reduced, in a similar manner to defective learning. The underlying mechanism, however, is different.

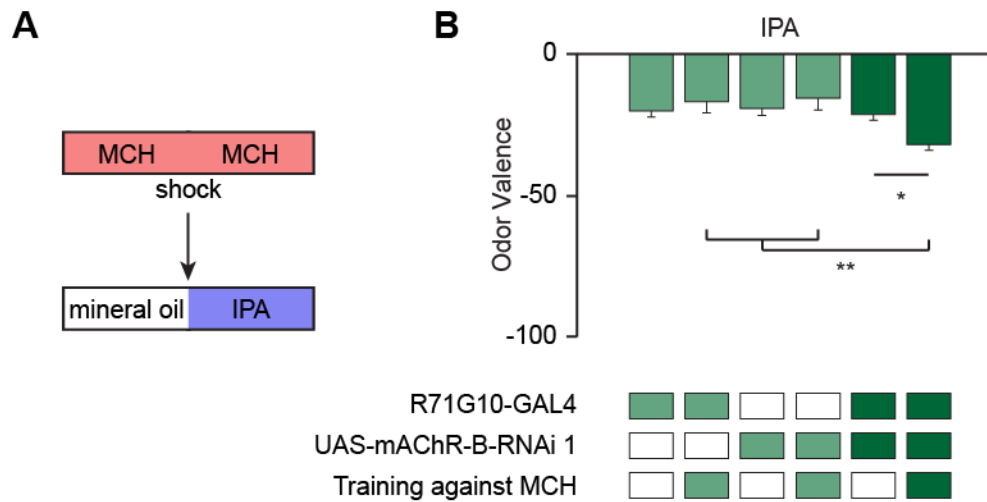


Figure S6: mAChR-B KD results in unspecific conditioning. Related to Figure 7.

A. Experimental protocol. Flies were conditioned against MCH using 12 equally spaced 1.25 s electric shocks at 50 V. Flies were then subjected to isopentyl acetate (IPA) for valence evaluation (see methods).

B. IPA valence observed with or without pre-exposure to conditioning against MCH in flies with mAChR-B RNAi 1 driven by R71G10-GAL4 (γ KCs). Following conditioning against MCH, mAChR-B KD flies showed increased aversion towards IPA whereas the parental controls showed reduced aversion towards IPA (mean \pm SEM), n (left to right): IPA: 77, 74, 75, 84, 84, 81; * $p < 0.05$, ** $p < 0.01$, *** $p < 0.001$; (Kruskal-Wallis Dunn's correction for multiple comparisons). For detailed statistical analysis see Table S1.

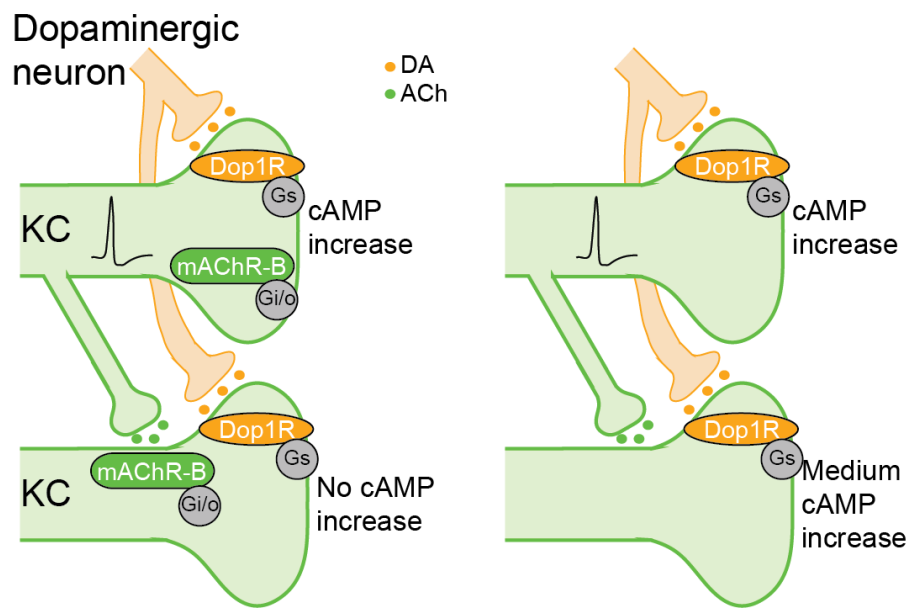


Figure S7: A model of mACHR-B lateral neuromodulation and noise free learning. Related to Figure 7.

Left, under normal conditions when pairing of an electric shock with an odor occurs, the CS⁺ activates a subset of KCs and DA is released on all KCs. DA coincidence with KC activity results in a large increase in cAMP (due to Ca²⁺ increase in KC presynaptic terminal, which is required for maximal activity of adenylate cyclase, top) and, as a result, induction of plasticity. DA also activates dopaminergic receptors on the less or non-active KCs (bottom). The active KCs release ACh, activating mACHR-B of their cognate KCs. This mACHR-B neuromodulation reduces cAMP and directly opposes the DA neuromodulation, resulting in suppression of cAMP increase in non-active KCs (bottom). In addition, mACHR-B decreases the Ca²⁺ elevation in KC presynaptic terminals. In the case of KCs that are non-active and weakly activate (and are therefore not the main carrier of the CS⁺ odor signal), this cholinergic neuromodulation will prevent DA neuromodulation (bottom). *Right*, when mACHR-B is KD, the high cAMP increase following DA in active KCs is not affected (top). However, in non-active and weakly active KCs there is no mACHR-B to counter the cAMP increase caused by DA. As a result, there is an increase in cAMP, even if to a lesser extent than that which occurs in active KCs. As a consequence, some plasticity occurs also in the off-target KCs. These KCs naturally do not respond reliably to the conditioned odor but rather to other odors. Thus, unspecific plasticity and conditioning can occur.